The Astronomical Journal, 148:89 (9pp), 2014 November doi:10.1088/0004-6256/148/5/89


# THE ENIGMA OF THE OPEN CLUSTER M29 (NGC 6913) SOLVED

V. Straižys[1], K. Milašius[1], R. P. Boyle[2], F. J. Vrba[3], U. Munari[4], N. R. Walborn[5], K. Černis[1], A. Kazlauskas[1], K. Zdanavičius[1], R. Janusz[6], J. Zdanavičius[1], and V. Laugalys[1]
[1] Institute of Theoretical Physics and Astronomy, Vilnius University, Goštauto 12, Vilnius LT-01108, Lithuania
[2] Vatican Observatory Research Group, Steward Observatory, Tucson, AZ 85721, USA
[3] U.S. Naval Observatory Flagstaff Station, P.O. Box 1149, Flagstaff, AZ 86002, USA
[4] INAF Astronomical Observatory of Padova, I-36012, Asiago (VI), Italy
[5] Space Telescope Science Institute, 3700 San Martin Drive, Baltimore, MD 21218, USA
[6] University School "Ignatianum," Cracow, Poland
*Received 2014 April 15; accepted 2014 July 17; published 2014 October 13*

## ABSTRACT

Determining the distance to the open cluster M29 (NGC 6913) has proven difficult, with distances determined by various authors differing by a factor of two or more. To solve this problem, we have initiated a new photometric investigation of the cluster in the Vilnius seven-color photometric system, supplementing it with available data in the *BV* and $JHK_s$ photometric systems and spectra of the nine brightest stars of spectral classes O and B. Photometric spectral classes and luminosities of 260 stars in a $15' \times 15'$ area down to $V = 19$ mag are used to investigate the interstellar extinction run with distance and to estimate the distance of the Great Cygnus Rift, $\sim 800$ pc. The interstellar reddening law in the optical and near-infrared regions is found to be close to normal, with the ratio of extinction to color excess $R_{BV} = 2.87$. The extinction $A_V$ of cluster members is between 2.5 and 3.8 mag, with a mean value of 2.97 mag, or $E_{B-V} = 1.03$. The average distance of eight stars of spectral types O9–B2 is $1.54 \pm 0.15$ kpc. Two stars from the seven brightest stars are field stars: HDE 229238 is a background B0.5 supergiant and HD 194378 is a foreground F star. In the intrinsic color–magnitude diagram, seven fainter stars of spectral classes B3–B8 are identified as possible members of the cluster. The 15 selected members of the cluster of spectral classes O9–B8 plotted on the $\log L/L_\odot$ versus $\log T_{\rm eff}$ diagram, together with the isochrones from the Padova database, give the age of the cluster as $5 \pm 1$ Myr.

*Key words:* open clusters and associations: individual (M29, NGC 6913, Cyg OB1) – stars: fundamental parameters

*Online-only material:* color figures, supplemental data

## 1. INTRODUCTION

Despite its impressive appearance, similar to a tiny Pleiades, the cluster M29 (NGC 6913) is a difficult object to understand. A glance at a deep exposure in blue or red filters shows that it is located in a small more transparent bay of a huge system of dark clouds known as the Great Cygnus Rift. Most prominent in the cluster are seven stars with *V* magnitudes 8.6–10.2, located within 5 arcmin: HD 194378, HDE 229221, HDE 229227, HDE 229234, HDE 229238, HDE 229239, and BD+38 4067. All of them are of O9–B0 spectral classes except for HD 194378, which is a known foreground F star.

The first evaluations of the cluster members and their distances were quite uncertain due to the low accuracy of photographic photometry, the lack of spectral and luminosity classifications, and of insufficient calibration accuracy of the photometric data (Zug 1933; Becker & Stock 1948; Tifft 1958). Tifft concluded that the cluster looked like it consisted of two groups at different distances—1.6 and 2.1 kpc. The brightest M29 stars were first classified in the MK system by Roman (1951); Morgan et al. (1953, 1955); Morgan & Harris (1956), and Hiltner (1956).

The next study of M29 was performed by Hoag et al. (1961), combining photoelectric and photographic *UBV* photometry. For the distance determination, a $V_0 - M_V$ versus $V_0$ diagram for B-type stars was used (Johnson 1960). Intrinsic $(B - V)_0$ values were found from the reddening-free parameters $Q_{UBV}$, and thus spectral types were not used. The mean extinction $A_V = 3.21$ mag and a distance of 1.15 kpc were found by Johnson et al. (1961). However, no explanations were given for how the cluster members were selected, and no mention of the group of the brightest stars of spectral types O9–B0 was given. It seems that these stars were ignored.

A few years later, Hoag & Applequist (1965) and Walker & Hodge (1968) obtained H$\gamma$ line photoelectric photometry of the brightest stars of M29 calibrated in absolute magnitudes. The distances to these stars were found to be much smaller than their spectroscopic distances. Crawford et al. (1977) using *uvby*H$\beta$ photometry found a similar result: the distances to the brightest stars calculated with the absolute magnitudes $M_V$, obtained from calibration of H$\beta$ absorption, were half of their spectroscopic distances. All this means that for the brightest M29 stars something was wrong either with their MK luminosity classes or with the calibration of the hydrogen line strengths in the luminosities.

Two subsequent investigations were aimed at increasing the number of stars in the vicinity of M29 with *UBV* photometry and MK spectral types. Joshi et al. (1983) have observed in *UBV* 103 stars covering the $40' \times 40'$ area for which the cluster membership probabilities from proper motions were estimated by Sanders (1973). Later on, most of these stars were classified in the MK system by Wang & Hu (2000) from low-resolution spectra.

The first $M_{\rm bol}$ versus $\log T_{\rm eff}$ HR diagram of M29 was obtained by Massey et al. (1995). Since the MK types were known only for the five brightest stars, other B and A stars were classified approximately by their $Q_{UBV}$ parameters. The age of the cluster from the comparison with isochrones, 4–6 Myr, mostly rests

# Report Documentation Page

*Form Approved*
*OMB No. 0704-0188*



| 1. REPORT DATE | 2. REPORT TYPE | 3. DATES COVERED |
|---|---|---|
| **NOV 2014** | | **00-00-2014 to 00-00-2014** |

| 4. TITLE AND SUBTITLE | 5a. CONTRACT NUMBER |
|---|---|
| **The Enigma Of The Open Cluster M29 (NGC 6913) Solved** | 5b. GRANT NUMBER |
| | 5c. PROGRAM ELEMENT NUMBER |
| 6. AUTHOR(S) | 5d. PROJECT NUMBER |
| | 5e. TASK NUMBER |
| | 5f. WORK UNIT NUMBER |
| 7. PERFORMING ORGANIZATION NAME(S) AND ADDRESS(ES) **U.S. Naval Observatory Flagstaff Station,,P.O. Box 1149,,Flagstaff,,AZ,86002** | 8. PERFORMING ORGANIZATION REPORT NUMBER |
| 9. SPONSORING/MONITORING AGENCY NAME(S) AND ADDRESS(ES) | 10. SPONSOR/MONITOR'S ACRONYM(S) |
| | 11. SPONSOR/MONITOR'S REPORT NUMBER(S) |

12. DISTRIBUTION/AVAILABILITY STATEMENT
**Approved for public release; distribution unlimited**

13. SUPPLEMENTARY NOTES
**The Astronomical Journal, 148:89 (9pp), 2014 November**

14. ABSTRACT

15. SUBJECT TERMS

| 16. SECURITY CLASSIFICATION OF: | | | 17. LIMITATION OF ABSTRACT | 18. NUMBER OF PAGES | 19a. NAME OF RESPONSIBLE PERSON |
|---|---|---|---|---|---|
| a. REPORT **unclassified** | b. ABSTRACT **unclassified** | c. THIS PAGE **unclassified** | **Same as Report (SAR)** | **10** | |

**Table 1**
Spectral Types of the Nine Brightest O9–B2 Stars of M29

| Paper I | HD, BD | Spectral type [Reference] | $V$ | $A_V$ | $d$ kpc |
|---|---|---|---|---|---|
| 943 | – | B2 V, SB [5]; B2 V [6] | 11.77 | 2.83 | 1.34 |
| 976 | 229221 | B0 II:e [1], B0pe [2], Be [3], B0.2 IIIe [4], B0 IIIe [5], B0:pe [6] | 9.22 | 3.41 | 1.45 |
| 1089 | 229227 | B0 III [1], B0 II [2], B0.2 III [3], O9.7 III [4], B0 V [5], O9.7 III(n) [6] | 9.34 | 3.06 | 1.80 |
| 1091 | – | B3 V [6] | 11.41 | 3.10 | 1.52 |
| 1123 | – | B1-1.5 V [6] | 11.91 | 3.83 | 1.64 |
| 1136 | +38 4067 | B0.2 III [3], B0 Ib/II [5], B0.5-0.7 V [6] | 10.20 | 3.00 | 1.55 |
| 1146 | 229234 | O9 II [1], O9.5 III [2], O9 If [3], O9 II [4], O9 Ib, SB [5], O9 III [6] | 8.91 | 3.03 | 1.64 |
| 1173 | 229238 | B0.5 II [1], B0.5 Ib [2], B0 I [3], B0.2 II [4], B0 I/II, SB [5], B0.5 Ia [6] | 8.86 | 3.10 | 3.56 |
| 1189 | 229239 | B0.5 IIe [1], B1 Iab [2], B0.5 IV [3], B0.2 III [4], B0 I, SB [5], B0.2 III [6] | 8.90 | 3.26 | 1.34 |

**References.** (1) Roman (1951); (2) Morgan et al. (1953, 1955); (3) Massey et al. (1995); (4) Negueruela (2004); (5) Boeche et al. (2004); (6) This paper.

on the five brightest stars, accepting their distance at 2.2 kpc. Later on, Liu et al. (1989) and Boeche et al. (2004) found that most of these stars are spectroscopic binaries exhibiting periodic variations of radial velocities.

From our review of photometric and spectroscopic investigations of M29, we conclude that the previous selection of cluster members is in question. Looking along the local spiral arm, the early-type stars can be found at all possible distances up to the edge of the arm at 4–5 kpc. Thus, the spectral class of a star without additional information about its distance is of little value for membership estimation. The MK typing of stars should be helpful, but, unfortunately, discrepancies among luminosity classes of O9–B0 stars are substantial. The reddening-free parameter $Q_{UBV}$ applied in some studies to identify B-type stars does not give luminosities, thus it is useless in estimating the membership. Also, a B-type star sample selected in this way can be contaminated by A and F stars. Proper motions of stars, used in some investigations as membership criteria, in the direction along the local spiral arm are too small to be useful at large distances. All these considerations lead to the conclusion that until now the cluster membership is the main problem that prevents determining an accurate distance to M29 and its age.

With the aim of identifying more early-type stars in the direction of M29 and to get more reliable information about their luminosities and distances, we decided to undertake a new investigation of the cluster in the Vilnius seven-color photometric system, which allows classification of most types of stars in spectral class and luminosity in the presence of variable interstellar reddening. Unfortunately, the system is not sufficiently sensitive to the luminosities of the stars of spectral classes O–B0, and thus we are not able to verify luminosity classes of the brightest stars of M29. Therefore, we decided to obtain new medium-resolution spectra of these stars in order to verify their luminosity classes.

## 2. SEVEN-COLOR PHOTOMETRY AND CLASSIFICATION

The results of CCD photometry in the Vilnius seven-color system, published by Milašius et al. (2013, hereafter Paper I), cover a 1.5 deg$^2$ area centered on the cluster at R.A. (J2000) = $20^{\rm h}24\overset{\rm m}{.}0$, decl. (J2000) = +38°30′. Magnitudes and colors were determined for 1752 stars down to $V = 19.5$ mag. However, the limiting magnitudes $V$ are not uniform in the whole area since three telescopes of different apertures and field sizes were used. The faintest stars have been measured in the central 13′ × 13′ area observed with the 1.8 m VATT telescope on Mt. Graham. A larger circular area with a 22′ diameter was observed with the 1 m telescope at the USNO Flagstaff Station down to a limiting magnitude of 17 mag. The largest 1.°25 square area was observed with the 35/51 cm Maksutov-type telescope of the Molėtai Observatory in Lithuania with a limiting magnitude of 15 mag. The magnitudes and colors of stars observed with the two or three telescopes were averaged. Standard stars used for the present photometry were observed in the Vilnius system photoelectrically by Kazlauskas & Jasevičius (1986).

The photometric data were used to classify about 70% of stars in spectral and luminosity classes and peculiarity types. The results of the classification are given in Paper I.

For this investigation of the cluster, we used the stars only in the central 15′ × 15′ area (Figure 1) that have been measured and classified to the faintest limiting magnitude.

The spectra of the nine brightest stars (Figure 2) were obtained with the 1.22 m telescope at the Asiago Observatory, equipped with a B&C spectrograph and a 600 lines/mm grating, providing a dispersion of 1.17 Å pixel$^{-1}$ and a resolving power of FWHM (PSF) = 2.1 pixel. The detector was an ANDOR iDus DU440A CCD with a 2048 × 512 array and 13.5 $\mu$m square pixels. The recorded wavelength range covers 3487–5885 Å. The nearby standard HR 8004 was used for the flux calibration. Data reduction in IRAF strictly followed the procedures described by Zwitter & Munari (2000) and involved all classical steps of correction for bias, dark, flat, sky background, and instrumental response. Spectral classification in the MK system was carried out by one of us (N.R.W.) using the standards from Walborn & Fitzpatrick (1990) and Sota et al. (2011). The classification results with comments are given below and in Table 1, which also gives the results of spectral classifications of other authors, based only on the slit spectra with a resolution comparable to or higher than that used for establishing the MK system, 125 Å mm$^{-1}$ at H$\gamma$ (Morgan et al. 1943).

*Star 1089*: O9.7 III(n). The ratio He II λ4541/Si III λ4552 ∼ 1 defines the spectral class. The ratio He II λ4686/He I λ4713 defines the luminosity class, in reasonable agreement with Si IV/He I near H$\delta$, which have broad lines. The λ4686/λ4713 ratio ∼1 would correspond to luminosity class II at this type, whereas it should be larger than it is for luminosity V. This ratio changes very rapidly between spectral classes of late O and B0, no doubt contributing to discrepancies in previous classifications. The broadening parameter is approximate, in the absence of standards.

*Star 1136*: B0.5–0.7 V. The ratio Si IV λ4089 ⩾ Si III λ4552 for spectral class. The luminosity class is based on He II λ4686 ∼ He I λ4713 at such a late type. O II and C III would favor a brighter luminosity class, but the helium line at λ4686 disallows

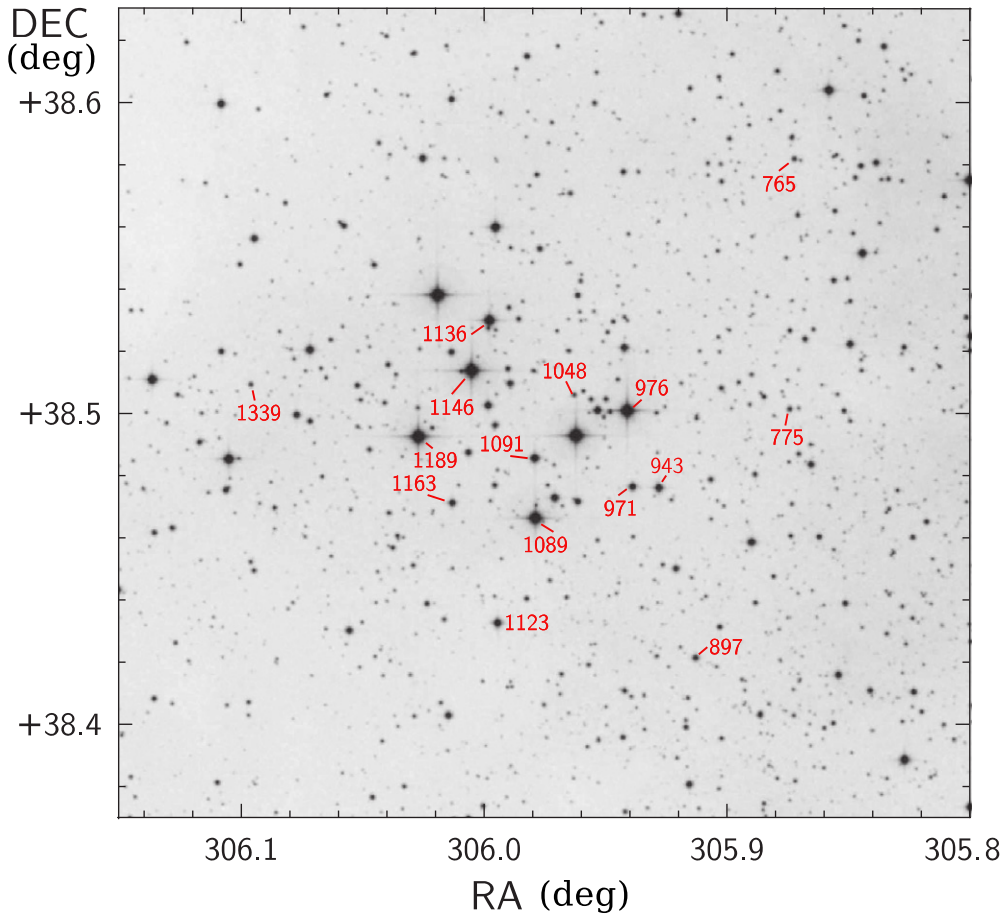


**Figure 1.** 15′ × 15′ field around the M29 cluster investigated in this study. The background image is the DSS2 Red image from SkyView. The numbered stars are 15 probable cluster members from Table 2. The numbers are from the catalog published in Paper I.

(A color version of this figure is available in the online journal.)

this. Of course, if composite (a possible interpretation), the classification is a compromise.

*Star 1146*: O9 III. The ratios He II λ4541 ∼ He I λ4387 and He II λ4200 ∼ He I λ4144 define the spectral class. The ratio He II λ4686/He I λ4713 defines luminosity class; the same remarks as for star 1089 above (except for good line quality here).

*Star 1173*: B0.5 Ia. Good match with $\kappa$ Ori in all criteria.

*Star 1189*: B0.2 III. Criteria are the same as above. Again, the fine divisions in spectral class are important, because if they are off, the luminosity class will be wrong since those criteria also evolve with the spectral classes.

The rest of the stars are classified with less confidence.

*Star 943*: B2 V.

*Star 976*: B0:pe. The absence of clear λ4200 and λ4541 eliminates earlier types, while C III λ4650 and He II λ4686 disfavor later ones. Luminosity classification is not realistic due to emission lines.

*Star 1091*: B2 V.

*Star 1123*: B1-1.5 V.

Luminosity classification at late-O and early-B types is difficult, because the luminosity criteria change very rapidly with spectral type, so that small errors (or uncertainties) in the latter entail large errors in the former and in the derived absolute magnitudes. New interpolated spectral types have been introduced to alleviate this problem (Sota et al. 2011, 2014). Also, there are some spectra with discrepancies between the Si IV/He I and He II/He I luminosity criteria, the resolution of which becomes arbitrary. Some of these problems are no doubt related to the endemic multiplicity of massive stars, in terms of both composite spectra and binary evolution. These issues likely contribute to discrepancies among different classifiers. They are extensively discussed by Walborn et al. (2014).

## 3. INTERSTELLAR REDDENING LAW

For the photometric classification of stars in the Vilnius system by interstellar reddening-free $Q$-parameters, the normal interstellar extinction law (see Straižys 1992) was applied. Since in the literature some authors discuss possible peculiarities of the reddening law in Cygnus, we have decided to verify the law by determining the slope of the interstellar reddening line in the $J - H$ versus $H - K_s$ diagram of the Two Micron All Sky Survey (2MASS) system (Skrutskie et al. 2006) and the ratios of color excesses $E_{V-m}/E_{B-V}$, where $m$ are the near-infrared magnitudes $J$, $H$, and $K$.

In the 15′ × 15′ area centered on M29, we selected 532 stars with $J$, $H$, $K_s$ accuracies of $\leqslant$0.05 mag. In Figure 3 we plot the $J - H$ versus $H - K_s$ colors for these stars and the intrinsic positions of the main sequence, red giant branch, and red clump giants (RCGs; central helium-burning stars) from Straižys & Lazauskaitė (2009). Also, the intrinsic line of the classical T Tauri stars from Meyer et al. (1997) and the reddening line for $Q_{JHK_s} = 0.0$ are shown. The classical T Tauri stars are usually

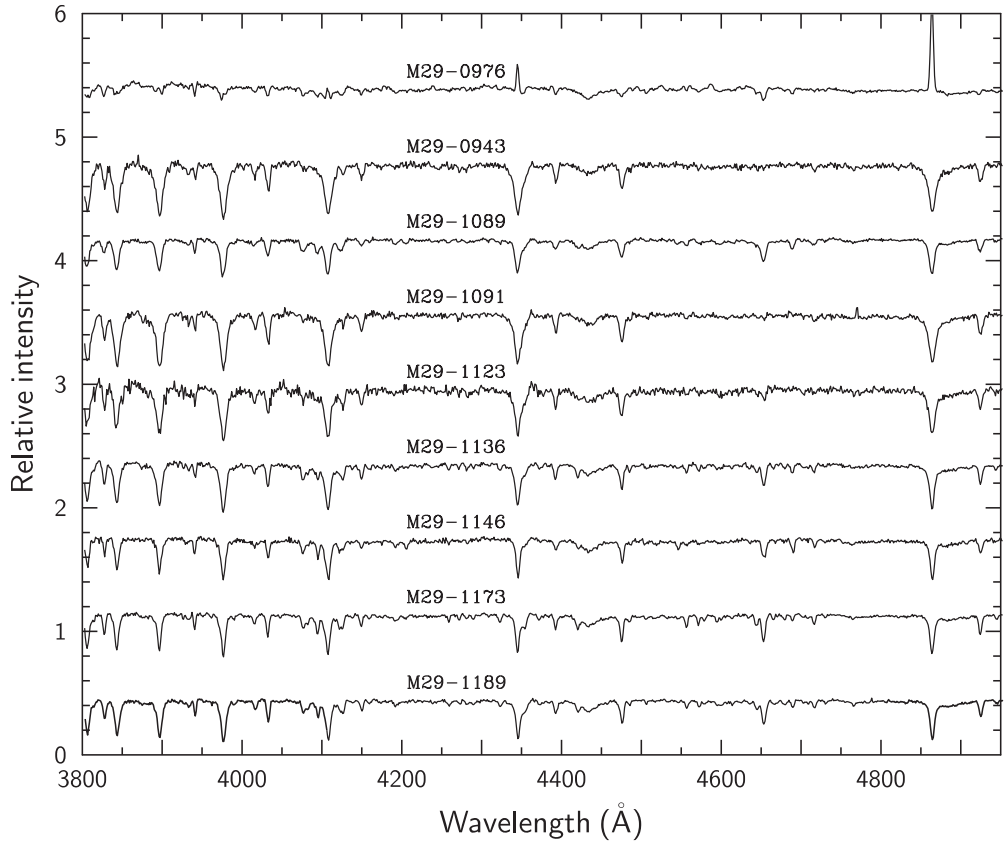


**Figure 2.** Spectra of nine M29 stars of spectral classes O and B obtained with the 1.22 m telescope of the Asiago Observatory. The numbers of the stars indicated correspond to the catalog by Milašius et al. (2013).

(Supplemental data of this figure are available in the online journal.)

located within the angle formed by these two lines. The reddened RCGs, together with normal (hydrogen-burning) red giants of spectral classes G5 to M5, form a common belt with a width of $\Delta\ (H - K_s) = 0.15$ mag; see Straižys & Laugalys (2009). However, in this belt, the RCGs should dominate since they outnumber by a factor of 10 the space density of normal giants (Perryman et al. 1995, 1997; Alves 2000).

In Figure 3, the reddening line of RCGs (with a certain amount of normal giants) can be drawn through their intrinsic position (the large open circle) and the middle of the belt above $J - H = 1.0$ (the broken line). We did not take stars in the belt lower than $J - H = 1.0$ since they are contaminated by stars of other luminosities with small reddenings. The slope of this line for 210 stars is $E_{J-H}/E_{H-K_s} = 2.044 \pm 0.080$. This slope is quite close to the normal value of 2.0 found in other galactic longitudes (Straižys et al. 2008; Straižys & Laugalys 2008). Thus, we will consider that in the direction of M29, the interstellar reddening law in the near-infrared wavelengths is close to normal.

Another test of the extinction law in the investigated area is the application of the ratio of color excesses $E_{V-J}/E_{B-V}$, $E_{V-H}/E_{B-V}$, and $E_{V-K}/E_{B-V}$ with the $J$, $H$, and $K$ magnitudes from 2MASS. For this aim, we used a list of B and A stars identified in the central $15' \times 15'$ area. Their $V$ and $B - V$ data were taken from Massey et al. (1995) and the AAVSO APASS survey, DR7,[7] and the near-infrared magnitudes from 2MASS. The ratios of color excesses were calculated separately for the Massey et al. (1995) and the APASS data and then transformed to the ratios $R_{BV} = A_V/E_{B-V}$ with the equations from Fitzpatrick (1999). The average value of $R_{BV}$ is found to be $2.87 \pm 0.16$, i.e., it is somewhat lower than a normal value of 3.15. This lower value corresponds to $R_{YV} = A_V/E_{Y-V} = 3.83$ in the Vilnius system (the normal value is 4.16).

According to Fitzpatrick & Massa (2007), there is no unique relation between the ratio $R_{BV}$ and the slope of the ultraviolet part of the extinction law. Thus, the lower value of $R_{BV}$ found in the area does not mean that the ratio of ultraviolet to visual color indices (for example $E_{U-B}/E_{B-V}$) should also be abnormal. To verify this, for photometric classification of stars in the area with interstellar reddening-free $Q$-parameters, we have applied the ratios of color excesses corresponding both to the normal and the so-called "Cygnus" law, with a somewhat smaller change of slope near the "knee" of interstellar extinction law at 4350 Å. The classification errors of individual stars were found to be lower in the case of the normal law.

## 4. INTERSTELLAR EXTINCTION

The 1.5 deg$^2$ area investigated in Paper I exhibits a very uneven density distribution of faint background stars since in this direction the line of sight is close to the edge of the Great Cygnus Rift dust clouds. The left side of the area is covered by the Rift clouds, and the right upper (northwestern) part of the area is the most transparent. The central area around the cluster and the lower part of the area exhibit an intermediate (although quite variable) obscuration. In the present paper, we investigated the extinction only in the $15' \times 15'$ area centered on the cluster.

[7] http://www.aavso.org/apass

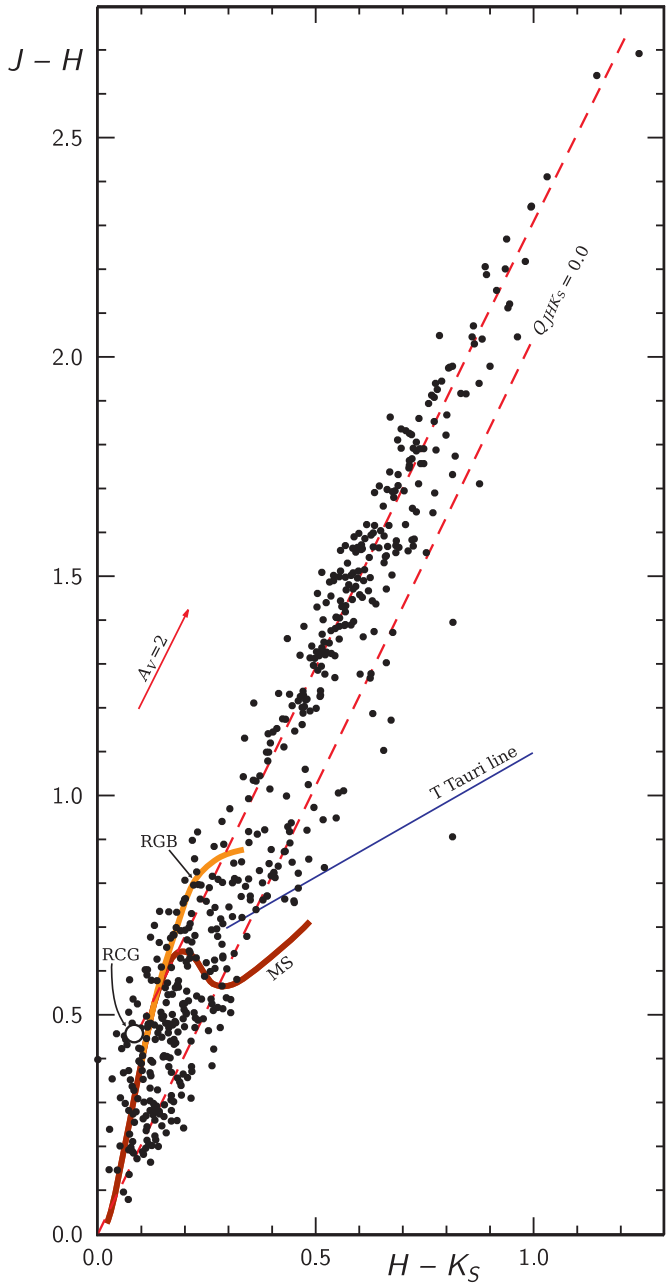


**Figure 3.** $J - H$ vs. $H - K_s$ diagram for 2MASS stars in the $15' \times 15'$ box centered on M29. The main sequence (MS, brown belt), red giant branch (RGB; orange belt), intrinsic locus of red clump giants (RCGs) with its reddening line, reddening line corresponding to $Q_{JHK_s} = 0$, and intrinsic T Tauri line are shown. (A color version of this figure is available in the online journal.)

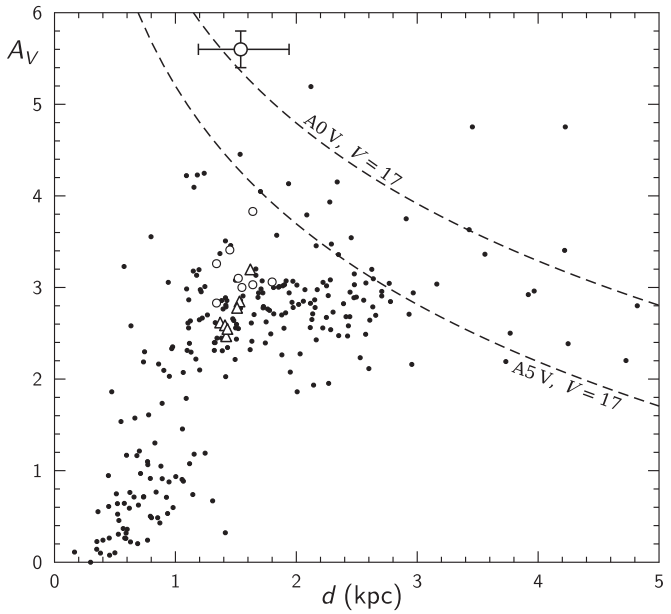


**Figure 4.** Extinction vs. distance diagram for the stars classified in MK spectral types in the $15' \times 15'$ area centered on the cluster. The probable cluster members classified spectroscopically are shown as open circles, and those classified photometrically as triangles. The two curves show the limiting magnitude effect for A0 V and A5 V stars at $V = 17$ mag. The cross showing the maximum ($3\sigma$) errors is shown at the distance of the cluster (1.54 kpc).

For the stars classified in the MK system, color excesses, extinctions, and distances were calculated with the equations

$$E_{Y-V} = (Y - V)_{\rm obs} - (Y - V)_0, \quad (1)$$

$$A_V = 3.83 E_{Y-V}, \quad (2)$$

$$\log d = 0.2(V - M_V + 5 - A_V), \quad (3)$$

where $(Y - V)_0$ and $M_V$ are the intrinsic color indices and absolute magnitudes for the corresponding MK types from Straižys (1992), with a correction of –0.1 mag to absolute magnitudes, adjusting their scale to the new distance modulus of the Hyades, $V - M_V = 3.3$ (Perryman et al. 1998). To calculate color excesses for O–B3 stars, spectroscopic MK types from this paper were used (see Table 1 in Section 2). For other stars, photometric spectral and luminosity classes were applied.

In Figure 4, we show the plot of the extinction $A_V$ versus distance $d$ in kpc for 260 stars in the $15' \times 15'$ area classified in the Vilnius system. The two curves in the upper right part of the diagram exhibit the limiting magnitude effect for A0 V and A5 V stars at $V = 17$ mag. We accepted this limiting magnitude because for fainter stars, the number of stars with a two-dimensional classification sharply decreases. These curves explain why the stars with high reddenings at large distances are absent. For example, above the curve corresponding to A0 V stars, only a few luminosity IV stars fainter than $V = 17$ mag have been observed and classified. The maximum ($3\sigma$) error cross is plotted at $d = 1.54$ kpc, the distance to the cluster that will be estimated in the next section. It corresponds to the distance errors for $\Delta M_V = \pm 0.5$ and the extinction errors $\pm 0.2$ mag.

The distribution of stars in Figure 4 shows a steep increase in extinction at about 500–600 pc to a value of ~3.5 mag. No doubt, this jump is related to the cloud system of the Great Cygnus Rift. In reality, the clouds are more distant than this rise in the extinction because of the negative distance errors of stars and the presence of stars with unresolved binarity. A typical error of absolute magnitude $M_V$ for B, A, and F stars of luminosity classes V–III, corresponding to one luminosity class, is about $\pm 0.5$, and this creates scatter in the calculated distances of stars to both sides by a factor of 1.26. This means that the distances of reddened stars, located apparently at 500 pc, must be multiplied by 1.26 to get the real distance of the cloud, 630 pc.

Another effect, which causes the shortward scatter of the apparent distances, is the unresolved binarity. If both components of such a binary are of the same luminosity, the real distance

of the binary should be larger by a factor of 1.41. This shifts the stars from 500 pc to 705 pc. If the luminosity difference of the components is larger, the expected shift will be smaller. If the unresolved binary has an additional shift shortward due to the negative luminosity error, the real distance to the front side of the cloud must be increased by a factor of $1.26 \times 1.41 = 1.78$. In this case, the real distance of the front side of the cloud is $500 \times 1.78 = 890$ pc. The conclusion is that the front side of the cloud is somewhere between 700 and 900 pc.

Figure 4 shows that the majority of stars concentrate in a relatively narrow band of $A_V$ between 2.4 and 3.2 mag. This means that behind the clouds of the Great Cygnus Rift, located at about 700–900 pc, the space is more or less free of dust, and this allows seeing stars up to 3 kpc with about the same extinction. The selected 15 cluster members (see Table 2 in Section 6) shown as open circles and triangles are located at apparent distances from 1.35 to 1.80 kpc. The extinction $A_V$ values of these 15 stars are very different (from 2.5 to 3.8 mag), and the average value is 2.97 mag, which corresponds to $E_{B-V} = 1.03$.

## 5. THE INTRINSIC COLOR–MAGNITUDE DIAGRAM

Since the age of M29 is expected to be of the order of a few million years, its color–magnitude diagram should contain zero-age main sequence (ZAMS) stars only in the B star range. The stars of lower masses should be on pre-main-sequence evolutionary tracks. The massive stars of early B subclasses are expected to show evolutionary deviations from the ZAMS.

For the determination of the cluster age, we must know which stars are the cluster members and what is their distance. If the cluster has a sufficiently abundant population representing a broad range of color indices, its distance can be easily estimated by fitting the ZAMS line to the lower envelope of the main sequence in the intrinsic (dereddened) color–magnitude diagram. However, the population of M29 is rather poor, and its main sequence in the color–magnitude diagram cannot be well distinguished from the field B–A stars located in the foreground and background.

The most natural way to determine the distance to M29 would be the use of the group of the six brightest stars without which the cluster would be hardly recognizable. Unfortunately, as was mentioned above, these stars are very problematic since their spectral types (especially luminosity classes) determined by different authors show considerable discrepancies; see Table 1.

For further analysis of the cluster, the spectral and luminosity classes determined from our spectra by N.R.W. were adopted. The extinctions and distances for these stars are given in the last two columns of Table 1. The absolute magnitude calibration of MK types was taken from Straižys (1992); the star 943 was considered to be a ZAMS star, and for the emission-line star 976, the luminosity class III was accepted. The ratio $R_{YV} = A_V/E_{Y-V} = 3.83$, corresponding to $R_{BV} = A_V/E_{B-V} = 2.87$, was applied (see Section 3).

Table 1 shows that almost all early-B stars in M29 except HDE 229238 exhibit similar distances, between 1.34 and 1.80 kpc, and their mean value is $1.54 \pm 0.15$ kpc (standard deviation). The errors of absolute magnitude, $\pm 0.5$ mag, at 1.54 kpc give the distance errors –0.32 kpc and +0.40 kpc. Since individual distances of the eight stars are contained within the distance error bars, we will consider them as being located at a mean distance of 1.54 kpc, which corresponds to the true distance modulus of 10.94 mag.

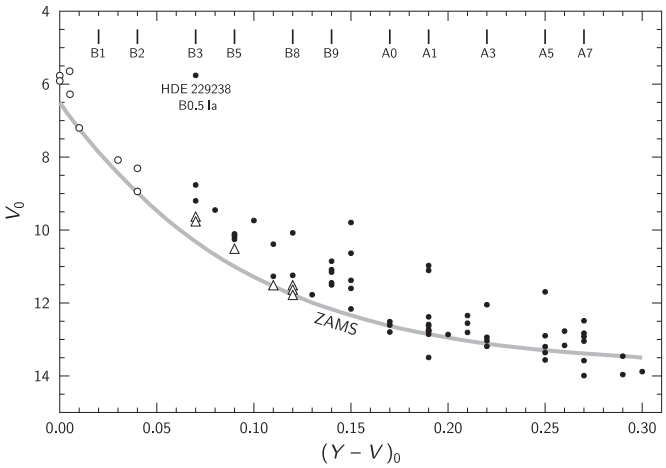


**Figure 5.** Intrinsic color–magnitude diagram for the O-B-A stars in the $15' \times 15'$ box in the Vilnius system. The probable members of M29 are shown as open circles (classified spectroscopically) and triangles (classified photometrically). The gray line is the ZAMS for a distance modulus of $V_0$–$M_V = 10.94$. The spectral classes for luminosity V–III stars corresponding to the intrinsic $Y - V$ values are shown at the upper axis.

Our next step is to estimate if more stars of cooler spectral types, B3–B8, located in the color–magnitude diagram close to the ZAMS, are present in the area within the same distance range (1.22–1.94 kpc). In Figure 5, we plot the intrinsic diagram $V_0$ versus $(Y - V)_0$ for stars of spectral classes O, B, and A in the $15' \times 15'$ area centered on the cluster. The ZAMS line shown is based on the Kazlauskas et al. (2006) table with small corrections originating from the PARSEC isochrones up to 12 $M_\odot$ (Bressan et al. 2012). The ZAMS line was extrapolated to larger masses (O8–B1 stars) with the older Padova isochrones (Bertelli et al. 1994; Girardi et al. 2002).

The five brightest stars with $V$ between 8.9 and 9.3, defining the visible cluster (after exclusion of the foreground star HD 194378), are located in the left upper corner of the diagram, close to $Y - V = 0$ and $V_0$ between 5.6 and 7.2 mag. Most of them are slightly above the ZAMS line.

In identifying possible ZAMS stars of the cluster with $Y - V > 0.03$ ($\geqslant$ B1), we should be cautious since these stars can be confused with the foreground and background field stars. Among the stars lying within 0.5 mag from the ZAMS and classified as luminosity V or IV–V stars, we have identified seven stars: 971 (B3), 1163 (B3), 897 (B5), 1339 (B7), 765 (B8), 775 (B8), and 1048 (B8). These stars (triangles in Figure 5) may also be cluster members; however, some of them can be unresolved binaries deviating upward from their single star positions. Taking their $M_V$ values for ZAMS, we get their distances from 1.37 kpc to 1.62 kpc, which within the errors are in agreement with the above estimated distance of M29 at 1.54 kpc. Luminosity classes of some of these stars from photometric classification have been obtained as V-IV, but this is not an argument against their attribution to ZAMS due to possible errors of colors and $Q$-parameters used in the classification. The cluster stars cooler than B8 are not expected to be close to the ZAMS line since for an age of the order of 5 Myr they should be pre-main-sequence objects. Some of them can be field stars.

The results reported above were based on Vilnius seven-color photometry. We have also verified if the same results can follow taking the observational data from the *B,V* photometric system. Table 2 contains 14 stars measured in *UBV* by Massey et al.

**Table 2**
Probable Members of the Cluster M29

| No. | $V$ | Sp | $(Y-V)_0$ | $E_{Y-V}$ | $A_V$ | $V_0$ | $M_V$ | $d$ kpc | BC | $\log T_{\rm eff}$ | $\log L/L_\odot$ | $p$(S) | $p$(D) |
|---|---|---|---|---|---|---|---|---|---|---|---|---|---|
| 765 | 14.18 | b8 Vz | 0.12 | 0.68 | 2.60 | 11.58 | 0.90 | 1.37 | −0.55 | 4.06 | 1.85 | | 96 |
| 775 | 14.12 | b8 Vz | 0.12 | 0.64 | 2.45 | 11.67 | 0.90 | 1.42 | −0.55 | 4.06 | 1.82 | | 95 |
| 897 | 13.12 | b5 Vz | 0.09 | 0.67 | 2.57 | 10.55 | −0.20 | 1.41 | −1.30 | 4.19 | 2.56 | 88 | 95 |
| 943 | 11.77 | B2 V, SB | 0.04 | 0.74 | 2.83 | 8.94 | −1.70 | 1.34 | −2.20 | 4.36 | 3.57 | | 95 |
| 971 | 12.21 | b3 Vz | 0.07 | 0.66 | 2.53 | 9.68 | −1.10 | 1.43 | −1.85 | 4.29 | 3.13 | 77 | 96 |
| 976 | 9.22 | B0 IIIe | 0.00 | 0.89 | 3.41 | 5.81 | −5.00 | 1.45 | −2.95 | 4.50 | 5.12 | 83 | 97 |
| 1048 | 14.65 | b8 Vz | 0.12 | 0.74 | 2.83 | 11.82 | 0.90 | 1.53 | −0.55 | 4.06 | 1.76 | | 82 |
| 1089 | 9.34 | B0 III, SB | 0.00 | 0.80 | 3.06 | 6.28 | −4.10 | 1.80 | −2.95 | 4.50 | 4.93 | 79 | 97 |
| 1091 | 11.41 | b2 V | 0.04 | 0.81 | 3.10 | 8.31 | −2.60 | 1.52 | −2.20 | 4.36 | 3.82 | 42 | 94 |
| 1123 | 11.91 | B1.5 V | 0.03 | 1.00 | 3.83 | 8.08 | −2.05 | 1.64 | −2.40 | 4.39 | 3.99 | 87 | 96 |
| 1136 | 10.20 | B0.5 V | 0.01 | 0.78 | 3.00 | 7.20 | −2.80 | 1.55 | −2.95 | 4.46 | 4.56 | 83 | 96 |
| 1146 | 8.91 | O9 III, SB | 0.00 | 0.79 | 3.03 | 5.88 | −5.20 | 1.64 | −3.15 | 4.52 | 5.17 | 78 | 97 |
| 1163 | 12.56 | b3 Vz | 0.07 | 0.72 | 2.76 | 9.80 | −1.10 | 1.51 | −1.85 | 4.29 | 3.08 | 88 | 96 |
| 1189 | 8.90 | B0 III, SB | 0.00 | 0.85 | 3.26 | 5.64 | −5.00 | 1.34 | −2.95 | 4.50 | 5.19 | 72 | 97 |
| 1339 | 14.73 | b7 Vz | 0.11 | 0.83 | 3.18 | 11.55 | 0.50 | 1.62 | −0.80 | 4.11 | 1.96 | | 96 |

**Notes.** The luminosity classes Vz correspond to ZAMS. In the last two columns, $p_{(S)}$ and $p_{(D)}$ mean the cluster membership probabilities (in percent) from Sanders (1973) and W. S. Dias (2013, private communication).

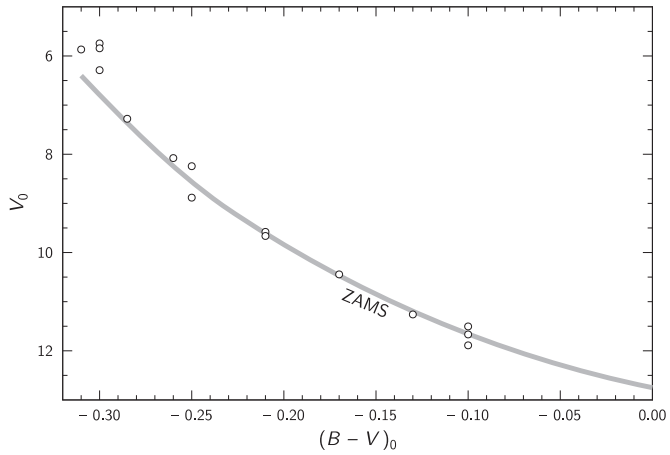


**Figure 6.** Intrinsic color–magnitude diagram in the $BV$ system for the 15 probable cluster members of spectral classes O9–B8. The gray line is the ZAMS for a distance modulus $V_0$–$M_V = 10.94$.

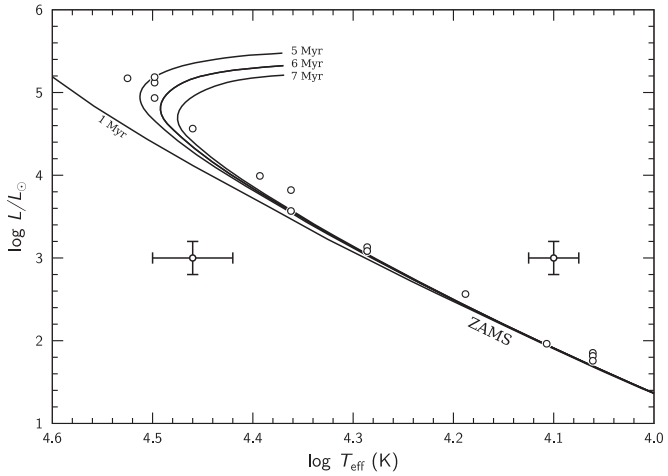


**Figure 7.** Effective temperature vs. luminosity diagram for the 15 probable members of the cluster and the Padova isochrones for the ages 1, 5, 6, and 7 Myr. The maximum ($3\sigma$) error crosses for the early and late B subclasses are shown.

(1995). The missing $BV$ data for the star 1339 were taken from Hoag et al. (1961). Their color excesses $E_{B-V}$ were calculated with the intrinsic colors from Straižys (1992). The ratio $R_{BV} = 2.87$, determined in Section 3, has been applied. The resulting intrinsic color–magnitude diagram $V_0$ versus $(B-V)_0$ is shown in Figure 6. Here, the ZAMS line is defined by combining the Padova isochrones for 1 and 10 Myr, and accepting the distance modulus $V_0$–$M_V = 10.94$. It is evident that the positions of stars in this diagram and the $V_0$ versus $(Y-V)_0$ diagram (Figure 5) are very similar. The stars between spectral classes B3 and B8 lie close to the ZAMS, while O9–B2 stars deviate to higher luminosities. Consequently, the two independent photometric data sets confirm that the cluster distance is really close to 1.5 kpc.

## 6. THE PHYSICAL HR DIAGRAM

The possible members of M29 of spectral classes O9–B8 are listed in Table 2. Figure 7 shows the $\log L/L_\odot$ versus $T_{\rm eff}$ diagram for these stars considering that they are located at 1.54 kpc ($V_0 - M_V = 10.94$). The isochrones plotted for the ages 1, 5, 6, and 7 Myr are taken from the Padova database of stellar evolutionary tracks and isochrones for the solar metallicity ($Z = 0.014$, Asplund et al. 2009).[8] The isochrones and the ZAMS line correspond to the basic set of the Padova isochrones up to masses of 120 $M_\odot$ (Girardi et al. 2002). Luminosities of stars in solar units were calculated with the equation

$$\begin{aligned}\log L/L_\odot &= 0.4(M_{\rm bol,\odot} - M_{\rm bol,\star}) \\ &= 0.4\,(4.72 - V + A_V + {\rm DM} - {\rm BC}), \end{aligned} \quad (4)$$

where $V$ is the apparent magnitude of the star, $M_{\rm bol,\star}$ is its absolute bolometric magnitude, $M_{\rm bol,\odot} = 4.72$ is the bolometric absolute magnitude of the Sun, BC is the bolometric correction, and DM is the true distance modulus of the cluster. The extinctions $A_V$ were determined with Equation (2). The DM in Figure 7 is taken as 10.94, which corresponds to a distance of 1.54 kpc. The effective temperatures and bolometric corrections were taken according to their spectral types from Straižys

[8] http://stev.oapd.inaf.it/cgi-bin/cmd

(1992). This $T_{\rm eff}$ scale for B stars is close to those given by Flower (1996), Bessell et al. (1998), and Torres (2010).

It is evident that at a distance of 1.54 kpc the five most massive members of M29 fit well with the 5 and 6 Myr isochrones. An age of $5 \pm 1$ Myr can probably be accepted. The fainter stars deviate from the ZAMS less than $\Delta \log L/L_{\odot} = 0.2$, which corresponds to 0.5 mag in absolute magnitude; thus, their positions within the errors do not contradict cluster membership. Their deviations from the ZAMS can be explained by the errors of (1) spectral or photometric classification, (2) calibration of MK types in terms of temperatures and BCs, (3) distance modulus determination, and (4) the isochrones themselves. Unresolved duplicity also cannot be excluded. Figure 7 shows the error bars for the early- and late-B subclasses. The errors in temperatures correspond to $\pm 0.5$ spectral subclass, and the errors in luminosities correspond to $\pm 0.5$ mag.

## 7. DISCUSSION

It seems that our investigation has solved the longstanding problem of the distance and age of the cluster M29. The main reason preventing determination of the cluster distance earlier is related to insufficient accuracy of the luminosity classifications of its brightest stars.

The luminosity class errors may originate from different reasons. The simplest source of error can be the differences in quality and resolving power between spectra of the program and the comparison stars, which can make the list of luminosity criteria inapplicable. The early classifications, in which the photographic method was used, could suffer from the sensitivity variations across the plates, i.e., insufficient "flat-fielding." Boeche et al. (2004) point also to a possible effect on the intensities of the compared lines that fall on different Echelle orders.

Therefore, it is important to have additional criteria for the determination of cluster membership. One such criterion might be the proper motions of stars in the cluster area. At present, proper motions of great numbers of stars are available in the astrometric catalogs, such as UCAC, PPMXL, and others. In the area of M29, proper motions determined by Sanders (1973) are available; however, their limiting magnitude is too shallow. As we mentioned in the Introduction, in the direction along the local spiral arm, proper motions are small, and their errors frequently are larger than the proper motions themselves. However, Table 2 shows that all the selected probable members have high membership probabilities given by Sanders (1973) and by W. S. Dias (2013, private communication), the latter determined from proper motions given in the UCAC4 catalog. Unfortunately, many stars that are definitely foreground and background stars also have membership probabilities close to 100. This means that proper motions are not sufficient to have trustworthy memberships. Radial velocities are much more informative (see NGC 6819; Tabetha Hole et al. 2009). According to Liu et al. (1989) and Boeche et al. (2004), the heliocentric velocity of M29 is –16.4 and –16.9 km $s^{-1}$, respectively. Boeche et al. find that seven stars from Table 2 (943, 976, 1089, 1123, 1136, 1146, and 1189) are radial velocity members. For the remaining eight stars, radial velocities have not been measured.

In this paper, the cluster members were identified mainly from their visible crowding and from spectroscopic and photometric distances. As the result, 15 member stars of M29 within the $15' \times 15'$ area centered on the cluster were selected. Many previous investigations have also used spectroscopic and photometric distances, but usually they showed a much larger dispersion and even bimodal distribution, originating from the errors in the luminosity classes of the most luminous stars. Also, in most of the previous papers, the normal value of the ratio $R = A_V/E_{B-V}$ has been applied. We have found that in the direction of M29 the ratio $R$ is lower than the standard value, and this resulted in a larger distance of the cluster stars by a factor of about 1.15. The range of extinctions for cluster members is in good agreement with the surrounding field stars (Figure 4).

Considering the cluster distance, the decisive factor was the application of the new MK spectral types of the brightest stars determined with the criteria developed by Walborn & Fitzpatrick (1990) and Sota et al. (2011) and applied to classification of O–B stars of M29 by N.R.W. himself. The results are in perfect agreement with the photometric data in the Vilnius and *B,V* systems and the Padova isochrones.

It may seem that a shortcoming in our distance and age determination is the neglect of spectroscopic binarity of the four O9–B0 stars discovered by Liu et al. (1989) and Boeche et al. (2004). If their components were of the same spectral type, the single stars should be fainter by 0.75 mag and more distant by a factor of 1.41. However, since the spectral lines of the secondaries are not observable, differences in magnitudes between the components should be much larger. In this respect, it is interesting to note that the exclusion of the four spectroscopic binaries from the distance determination does not change the mean distance itself—it remains 1.54 kpc. A small vertical shift of the binaries down in the HR diagram also does not change the estimate of the age, since isochrones in the range of O9–B1 spectral types run almost vertically.

The intrinsic color–magnitude diagram in Figure 5 shows that there are a number of stars in the B3–A7 range lying above the ZAMS up to 2.5 mag. Some of them could be field stars and others could be binary stars of the cluster. Distances and reddenings of some of these stars with luminosities IV and III allow them to be the evolved cluster members. This could imply that star formation in the cluster began about 50 Myr ago and is still ongoing. While this is not impossible, we note the absence of a prestellar dust and gas cloud in the cluster vicinity. Most probably, the main star-forming activity in the cluster took place about 5–6 Myr ago, and after that the massive luminous O–B stars dissipated the remains of the parent cloud.

If the low-mass young stellar objects (YSOs) were formed at the same time as the massive ones, they should be present in the area of M29. We estimated the apparent magnitudes of possible T Tauri stars of spectral type K in M29, comparing it with the cluster NGC 2264, which is of a similar age and contains pre-main-sequence stars of both high and low masses. In this cluster, pre-main-sequence stars of early-K subclasses appear at $V =$ 13.5 mag (Park et al. 2000). Since the distance to NGC 2264 is 760 pc (Dahm 2008), the difference of the true distance moduli of both clusters is 1.54 mag. The mean extinctions $A_V$ are 0.2 mag for NGC 2264 and ~3 mag for M29. Consequently, the difference of the apparent distance moduli of both clusters is about 4.3 mag. The conclusion is that in M29, YSOs of class II and spectral class K are expected to be fainter than $V$ about 17.8 mag or $J$ about 16.4 mag. This means that in M29, YSOs of class II should be invisible in 2MASS photometry (see the limiting magnitudes in Skrutskie et al. (2006)) but they should be easily detectable in the UKIDSS survey (Lucas et al. 2008). In the UKIDSS $J - H$ versus $H - K$ diagram of the area, tens

of sources above the intrinsic T Tauri line are seen, but their identification as YSOs of M29 is problematic. A special study, using the data from the UKIDSS, *Spitzer*, *WISE*, IPHAS, and other surveys, is essential.

The M29 cluster is usually considered to be a member of the Cyg OB1 association, along with the clusters IC 4996, Berkeley 86, and Berkeley 87; see the recent review by Reipurth & Schneider (2008). Other than the clusters, the association contains tens of O–B3 stars and cooler supergiants scattered in an area of $4^\circ \times 3\overset{\circ}{.}5$ (Humphreys 1978; Garmany & Stencel 1992). The distance to this association is still controversial but is usually considered to be 1.3–1.5 kpc. The distance to the cluster M29 determined in this investigation is close to the largest of these distances. According to Hanson (2003), the massive association Cyg OB2 located $\sim 3^\circ$ north of M29 can be also located at the same distance. In this case, the centers of Cyg OB2 and M29 are separated by ~80 pc. However, both star groups probably are not physically related since their movements are somewhat different: the heliocentric radial velocity is –10.3 km s$^{-1}$ for Cyg OB2 (Kiminki et al. 2007) and –16.9 km s$^{-1}$ for M29 (Boeche et al. 2004).

## 8. RESULTS AND CONCLUSIONS

This investigation is based on the results of seven-color photometry and two-dimensional classification of 260 stars down to $V \approx 19$ mag in a $15' \times 15'$ area centered on the cluster M29 (NGC 6913), 2MASS $JHK_s$ photometry, and the blue spectra for the nine brightest stars of M29 obtained at the Asiago Observatory. The spectra were classified in spectral and luminosity classes with the criteria described by Walborn & Fitzpatrick (1990) and Sota et al. (2011). The following results were obtained.

1. The ratio of color excesses is found to be $E_{J-H}/E_{H-K_s} = 2.044 \pm 0.080$. This means that the interstellar extinction law in the near-infrared spectral range is close to normal. However, the ratio $R = A_V/E_{B-V}$, found from the ratios $E_{V-i}/E_{B-V}$ for the $i = J$, $H$, and $K_s$ passbands, is close to 2.87, i.e., somewhat lower than the normal value $R = 3.15$. In the violet and ultraviolet spectrum down to 300 nm, the normal interstellar extinction law is valid again.
2. The distance to M29, $1.54 \pm 0.15$ kpc, is determined as the average of the distances of eight stars of spectral types O9–B2 classified from the Asiago spectra. Two stars from the seven brightest ones are found to be field stars: HDE 229238 is a background B0.5 supergiant and HD 194378 is a foreground F star.
3. In the intrinsic color–magnitude diagram of O-B-A stars, we selected seven more stars of spectral classes B3–B8 lying close to the ZAMS, which may also be considered cluster members. The cooler stars were not considered since they should still be in the pre-main-sequence stage of evolution.
4. The 15 probable members of the cluster of spectral classes O9–B8, plotted on the $\log L/L_\odot$ versus $\log T_{\rm eff}$ diagram together with the isochrones from the Padova database, give an age of the cluster $5 \pm 1$ Myr. The extinction $A_V$ is variable across the cluster (from 2.5 to 3.8 mag), the average value being 2.97 mag, which corresponds to $E_{B-V} = 1.03$.
5. The distances to the clouds of the Great Cygnus Rift are estimated to be in the range of 700–900 pc.

Use of the Simbad, WEBDA, ADS, SkyView, 2MASS, and UKIDSS databases is acknowledged. We are grateful to Wilton S. Dias for membership probabilities in the M29 area presented before publication. The paper is partly supported by the Research Council of Lithuania, grant No. MIP-061/2013.

## REFERENCES

Alves, D. R. 2000, ApJ, 539, 732
Asplund, M., Grevesse, N., Sauval, A. J., & Scott, P. 2009, ARA&A, 47, 481
Becker, W., & Stock, J. 1948, AN, 278, 115
Bertelli, G., Bressan, A., Chiosi, C., et al. 1994, A&AS, 106, 275
Bessell, M. S., Castelli, F., & Plez, B. 1998, A&A, 333, 231
Boeche, C., Munari, U., Tomasella, L., & Barbon, R. 2004, A&A, 415, 145
Bressan, A., Marigo, P., Girardi, L., et al. 2012, MNRAS, 427, 127
Crawford, D. L., Barnes, J. V., & Hill, G. 1977, AJ, 82, 606
Dahm, S. E. 2008, in Handbook of Star Forming Regions, Vol. 1, ed. B. Reipurth (San Francisco, CA: ASP), 966
Fitzpatrick, E. L. 1999, PASP, 111, 63
Fitzpatrick, E. L., & Massa, D. 2007, ApJ, 663, 320
Flower, P. J. 1996, ApJ, 469, 355
Garmany, C. D., & Stencel, R. E. 1992, A&AS, 94, 211
Girardi, L., Bertelli, G., Bressan, A., et al. 2002, A&A, 391, 195
Hanson, M. M. 2003, ApJ, 597, 957
Hiltner, W. A. 1956, ApJS, 2, 389
Hoag, A. A., & Applequist, N. L. 1965, ApJS, 12, 215
Hoag, A. A., Johnson, H. L., Iriarte, B., et al. 1961, PUSNO, 17, 349
Humphreys, V. R. M. 1978, ApJS, 38, 309
Johnson, H. L. 1960, LowOB, 5, 17
Johnson, H. L., Hoag, A. A., Iriarte, B., et al. 1961, LowOB, 5, 133
Joshi, U. C., Sanwal, B. B., & Sagar, R. 1983, PASJ, 35, 405
Kazlauskas, A., & Jasevičius, V. 1986, VilOB, 75, 18
Kazlauskas, A., Straižys, V., Bartašiūtė, S., et al. 2006, BaltA, 15, 511
Kiminki, D. C., Kobulnicky, H. A., Kinemuchi, K., et al. 2007, ApJ, 664, 1102
Liu, T., Janes, K. A., & Bania, T. M. 1989, AJ, 98, 626
Lucas, P. W., Hoare, M. G., Longmore, A., et al. 2008, MNRAS, 391, 136
Massey, P., Johnson, K. E., & DeGioia-Eastwood, K. 1995, ApJ, 454, 151
Meyer, M. R., Calvert, N., & Hillenbrand, L. A. 1997, AJ, 114, 288
Milašius, K., Boyle, R. P., Vrba, F. J., et al. 2013, BaltA, 22, 181 (Paper I)
Morgan, W. W., Code, A. D., & Whitford, A. E. 1955, ApJS, 2, 41
Morgan, W. W., & Harris, D. L. 1956, VA, 2, 1124
Morgan, W. W., Keenan, P. C., & Kellman, E. 1943, An Atlas of Stellar Spectra (Chicago, IL: Univ. Chicago Press)
Morgan, W. W., Whitford, A. E., & Code, A. D. 1953, ApJ, 118, 318
Negueruela, I. 2004, AN, 325, 380
Park, B.-G., Sung, H., Bessell, M. S., & Kang, Y. H. 2000, AJ, 120, 894
Perryman, M. A. C., Brown, A. G. A., Lebreton, Y., et al. 1998, A&A, 331, 81
Perryman, M. A. C., Lindegren, L., Kovalevsky, J., et al. 1995, A&A, 304, 69
Perryman, M. A. C., Lindegren, L., Kovalevsky, J., et al. 1997, A&A, 323, L49
Reipurth, B., & Schneider, N. 2008, in Handbook of Star Forming Regions, Vol. 1, ed. B. Reipurth, ASP, 36
Roman, N. G. 1951, ApJ, 114, 492
Sanders, W. L. 1973, A&AS, 9, 221
Skrutskie, M. F., Cutri, R. M., Stiening, R., et al. 2006, AJ, 131, 1163
Sota, A., Maíz Apellániz, J., Morrell, N. I., et al. 2014, ApJS, 211, 10
Sota, A., Maíz Apellániz, J., Walborn, N. R., et al. 2011, ApJS, 193, 24
Straižys, V. 1992, Multicolor Stellar Photometry (Tucson, AZ: Pachart Publishing House), http://www.itpa.lt/MulticolorStellarPhotometry/
Straižys, V., Corbally, C. J., & Laugalys, V. 2008, BaltA, 17, 125
Straižys, V., & Laugalys, V. 2008, BaltA, 17, 253
Straižys, V., & Laugalys, V. 2009, BaltA, 18, 141
Straižys, V., & Lazauskaitė, R. 2009, BaltA, 18, 19
Tabetha Hole, K., Geller, A. M., Mathieu, R. D., et al. 2009, AJ, 138, 159
Tifft, W. G. 1958, AJ, 63, 127
Torres, G. 2010, AJ, 140, 1158
Walborn, N. R., & Fitzpatrick, E. L. 1990, PASP, 102, 379
Walborn, N. R., Sana, H., Simón-Díaz, S., et al. 2014, A&A, 564, A40
Walker, G. A. H., & Hodge, S. M. 1968, PASP, 80, 290
Wang, J.-J., & Hu, J.-Y. 2000, A&A, 356, 118
Zug, R. S. 1933, LicOB, 16, 119
Zwitter, T., & Munari, U. 2000, An Introduction to Analysis of Single Dispersion Spectra with IRAF, Asiago Monografie, Vol. 1, Padova